078900-1-F

THE UNIVERSITY OF MICHIGAN

COLLEGE OF ENGINEERING
DEPARTMENT OF ELECTRICAL & COMPUTER ENGINEERING
SPACE PHYSICS RESEARCH LABORATORY

FINAL REPORT

OGO-E-02 DATA ANALYSIS

PREPARED ON BEHALF OF THE PROJECT BY

A. F. NAGY

W. M. SILVIS

E. C. FOUST

UNDER CONTRACT WITH:

NATIONAL AERONAUTICS AND SPACE ADMINISTRATION
GODDARD SPACE FLIGHT CENTER
CONTRACT NO. NAS5-9306
GREENBELT, MARYLAND

OFFICE OF RESEARCH ADMINISTRATION · ANN ARBOR

THE UNIVERSITY OF MICHIGAN

COLLEGE OF ENGINEERING
Department of Electrical & Computer Engineering
Space Physics Research Laboratory

Final Report

OGO-F-02 DATA ANALYSIS

Prepared on behalf of the project by

A. F. NAGY

W. M. SILVIS

E. C. FOUST

ORA Project 078900

under contract with:

NATIONAL AERONAUTICS AND SPACE ADMINISTRATION
GODDARD SPACE FLIGHT CENTER
CONTRACT NO. NAS5-9306
GREENBELT, MARYLAND

administered through:

OFFICE OF RESEARCH ADMINISTRATION ANN ARBOR

November 1972

TABLE OF CONTENTS

LIST OF ILLUSTRATIONS

1. INTRODUCTION

The OGO-VI satellite, which was launched on June 5, 1969 carried a complement of twenty-six experiments. One of those instruments, the F-02 package, was a cylindrical Langmuir probe experiment whose primary purpose was to measure ionospheric electron temperatures and densities. This report briefly describes the F-02 experiment itself, outlines the computer programs developed at The University of Michigan to analyze the raw data, and gives a summary of the scientific information obtained, so far, with the aid of this experiment.

2. EXPERIMENT DESCRIPTION

Cylindrical Langmuir probes have been used successfully for nearly a decade to measure electron temperatures and densities in the ionosphere (e.g. Brace, et al., 1963; Taylor, et al., 1963; Nagy, et al., 1963; Spencer, et al., 1965; Brace, et al., 1971). The theory of cylindrical Langmuir probes was first published nealy half a century ago by Mott-Smith and Langmuir (1926). More recently, this theory was extended to moving probes by Kanal (1964). The rocket- and satellite-borne instrumentation associated with these probes has been discussed extensively in the open literature (see Brace, et al., 1971).

The two cylindrical probes used on OGO-VI were mounted on the OPEP at right angles to each other as indicated in Figure 1. Each probe assembly consisted of a collector 9 in. long and 0.022 in. in diameter, and a concentric guard 9 in. long and 0.065 in. in diameter. The guard and the collector were made of stainless steel, and teflon was used as an insulator between them. The potentials of both the guard and the collector were driven together, but only the current to the collector was monitored. The purpose of the guard was twofold: 1) to keep the collector physically away from the OPEP surfaces, and 2) to help maintain a uniform field around the collector. A large portion of the OPEP surface was covered with a fine mesh gold-plated grid in order to insure a uniform sheath about the OPEP and to increase the "current dump" area of the spacecraft.

The electronics package was housed in the main body of the spacecraft. It consisted of a two-range logarithmic current detector and ramp voltage generator system (System I), a four-range linear current detector and ramp voltage generator system (System II), and a common control system shown in Figure 2. Tables I and II give many of the details of the characteristics of Systems I and II respectively, while Table III gives the command status indications.

The current detector in System I is a two-range differential one which has the following transfer functions:

$$e_{out} = 2 \log_{10} (3160\ I_p + 1)$$

$$e_{out} = 2 \log_{10} (31.6\ I_p + 1)$$

where e_{out} and I_p are in volts and microamperes, respectively. The detector ranges alternate with each ramp voltage sweep. The ramp voltage is a linear 6 V sweep with a period of 9.2 sec for normal operation and 2.3 sec in the fast format mode of operation.

A spacecraft will acquire some variable negative potential with respect to the plasma. The probes have to be swept both positive and negative with respect to the plasma and therefore it is desirable to be able to adjust the starting voltage of the ramp voltage sweep. In System I a special circuit which adjusts the ramp voltage bias is used to achieve this. At the beginning of each sweep the bias is automatically adjusted until the detector output is zero. The ramp voltage then sweeps from -2.5 V to +3.5 V with respect to this zero current (floating) potential. Thus the magnitude of the sweep is always 6 V but the starting point is allowed to vary from -4.5 V to +7.5 V, depending on the spacecraft potential.

The output of System I consists of three 144 msec (36 msec in fast format) bits followed by a voltage which is proportional to the logarithm of the collector current. The three 144 msec bits carry the following information: 1) ramp voltage retrace, 2) range, probe, and calibration information, and 3) the ramp start voltage. The system was normally operated with a 9.2 sec ramp voltage period with measurements alternating sequentially between probes 1 and 2. The system could be switched to fast format (2.3 sec period), and/or to measurements with one of the probes only.

An in-flight calibration took place approximately every ten minutes. During the calibration sequence a known resistor was attached to the input of the current detector to simulate full scale detector current. During this calibration period a complete ramp voltage sweep was also placed on the data output line to allow the ramp voltage to be monitored directly.

System II is quite similar to System I in operation but much simpler. System II utilizes a four-range differential current detector and produces as its output a voltage proportional to the collected probe current. The appropriate transfer functions are the following:

$$e_{out} = 1.54 + 350 \quad I_p$$

$$e_{out} = 1.54 + \quad 50 \quad I_p$$

$$e_{out} = 1.54 + 7.01 \; I_p$$

$$e_{out} = 1.54 + 1.0 \quad I_p$$

where e_{out} and I_p are in volts and microamperes, respectively. The detector changes ranges after each ramp voltage period which is 9.2 sec under normal operation and 2.3 sec during fast format operation.

This system does not have an automatically self-adjusting ramp starting voltage like that of System I; in this system the ramp voltage sweeps linearly from -3.5 V to 2.5 V with respect to a bias voltage level (one of the six bias levels, namely 0 V, 2 V, 4 V, 6 V, 8 V, 10 V, was selected by impulse command during the operation of System II). The format of the data output from this system is identical to that of System I: three information bits followed by probe current for each sweep. The bits carry the same information as indicated for System I. The calibration period for this system also occurs approximately every 10 minutes, and consists of zero current checks followed by detector current outputs due to appropriate resistors being placed across the input terminals in order to simulate full scale currents. During the final portion of the calibration sequence the ramp voltage is monitored directly.

Data from the subcom provided all the needed information for the impulse and power command status of both experiments. The details of the subcom monitor are shown in Table III.

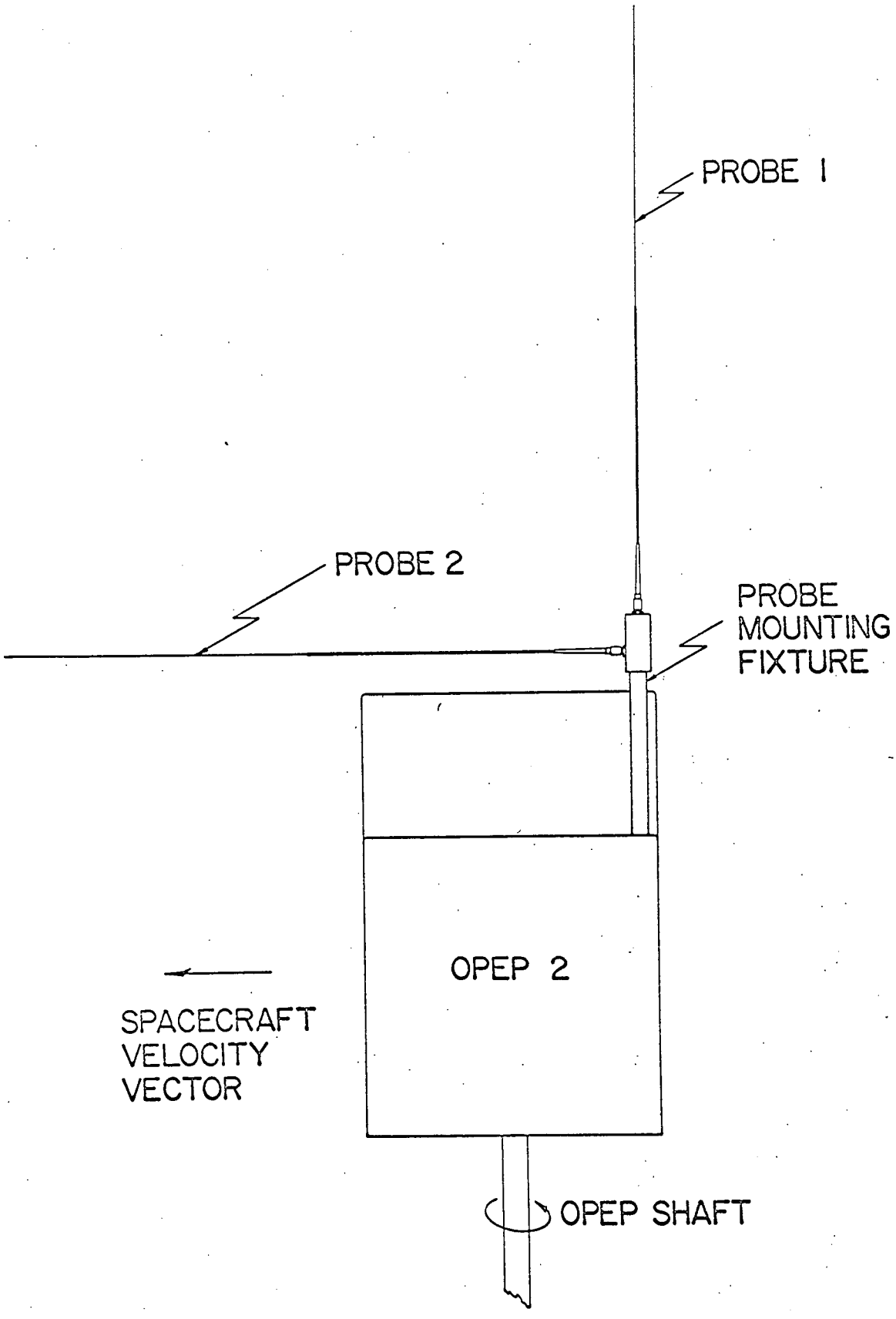

Figure 1. OGO-F-02 probe mounting configuration.

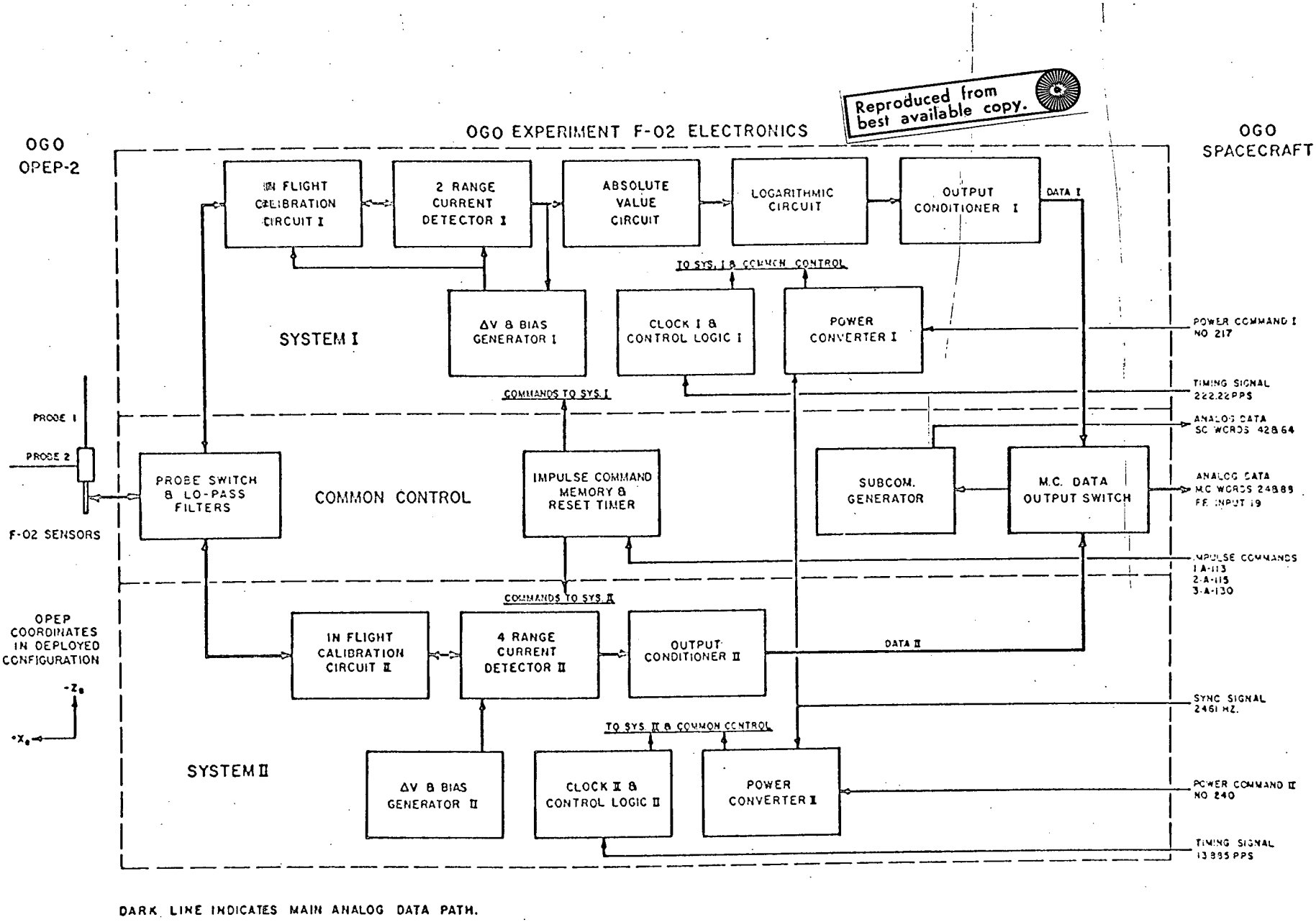

DARK LINE INDICATES MAIN ANALOG DATA PATH.

Figure 2. Block diagram, control system.

TABLE I

SYSTEM I CHARACTERISTICS

Sensitivities (Full Scale) Range 1 0.1×10^{-6}A

Range 2 10×10^{-6}A

Power 28 Vdc 2.24 W

(21.5 to 50 Vdc)

ΔV_{app} Normal Format -2.5 V to +3.5 V + Bias*

$\frac{dV}{dt}$ = .682 V/sec

Fast Format -2.5 V to +3.5 V + Bias*

$\frac{dV}{dt}$ = 2.728 V/sec

Sweep Characteristics

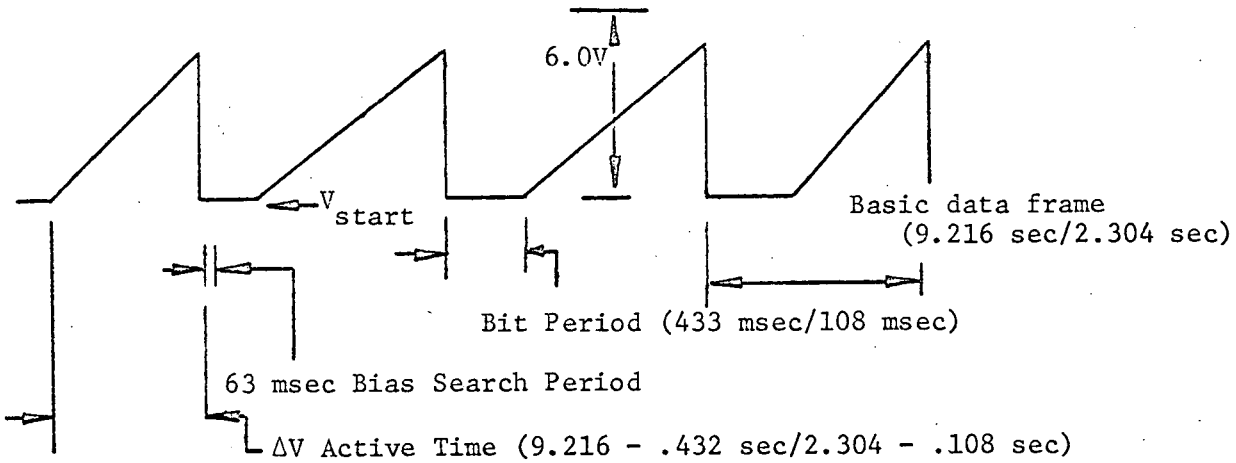

Detector Characteristics

Range 1

0.1 μA full scale

$e_{out} = 2 \log_{10} \{3160 \text{ V}/\mu\text{A} | I_p(\mu\text{A}) | + 1\}$

*Bias is V_{app} for zero net probe current ±100 mV; it is searched at each retrace time.

TABLE I (Continued)

Range 2

10 μA full scale

$e_{out} = 2 \log_{10} \{31.6 \text{ V/μA} |I_p(\text{μA})| + 1\}$

Output Characteristics

Data Output

$z_o = 10^3\ \Omega$

Data Limited at 4.95 V

Format (Time scale exaggerated)

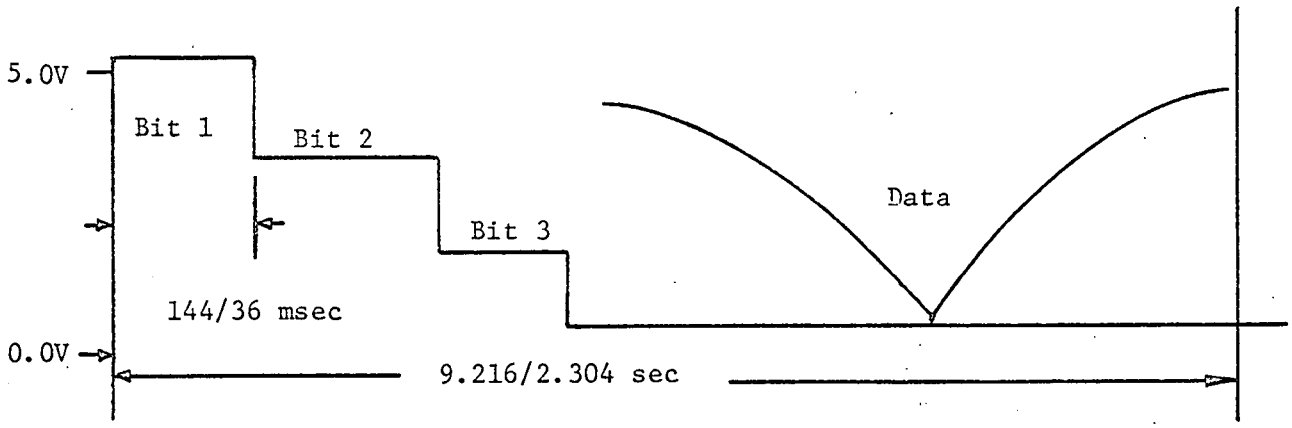

Bit 1 SYNC BIT, ALWAYS 5.1 V

Bit 2 RANGE, PROBE, CALIBRATE BIT

VOLTAGE	FUNCTION		
0.5	MEASURE	PROBE 2	RANGE 2
1.0	"	" 1	" 2
1.5	"	" 2	" 1
2.0	"	" 1	" 1
2.5	CALIBRATE	" 2	" 2
3.0	"	" 1	" 2
3.5	"	" 2	" 1
4.0	"	" 1	" 1

TABLE I (Concluded)

Bit 3 SWEEP VOLTAGE START BIT

FLIGHT UNIT:

SWEEP VOLTAGE START = 2.666 (Bit 3) - 4.909

TABLE II

SYSTEM II CHARACTERISTICS

Sensitivities (Full Scale)	Range 1	0.01 μA
	Range 2	0.07 μA
	Range 3	0.5 μA
	Range 4	3.5 μA

Power 28 Vdc at 1.88 W
(21.5 to 50 Vdc)

ΔV_{app} -3.5 V to +2.5 V + Bias*

$\frac{dV}{dt}$ = .682 V/sec

*Bias is 0V, 2V, 4V, 6V, or 10V depending on command status.

Sweep Characteristics

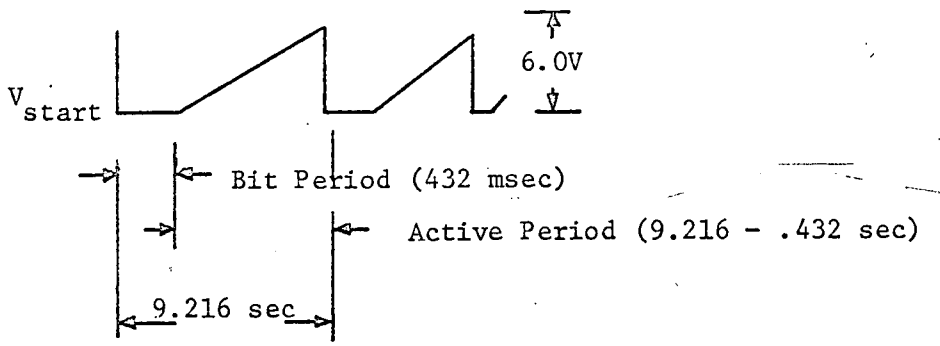

Detector Characteristics

Range 1

0.01 μA full scale

e_{out} = 1.54 V + 350 V/μA(I_p(μA))

TABLE II (Continued)

Range 2

0.07 μA full scale

e_{out} = 1.54 V + 50.0 V/μA(I_p(μA))

Range 3

0.5 μA full scale

e_{out} = 1.54 V + 7.01 V/μA(I_p(μA))

Range 4

3.5 μA full scale

e_{out} = 1.54 V + 1.00 V/μA(I_p(μA))

Output Characterisitcs

Data Output

$z_o = 10^3\ \Omega$

Data Limited at 4.95 V Negative Clamp at -0.6 V

Format

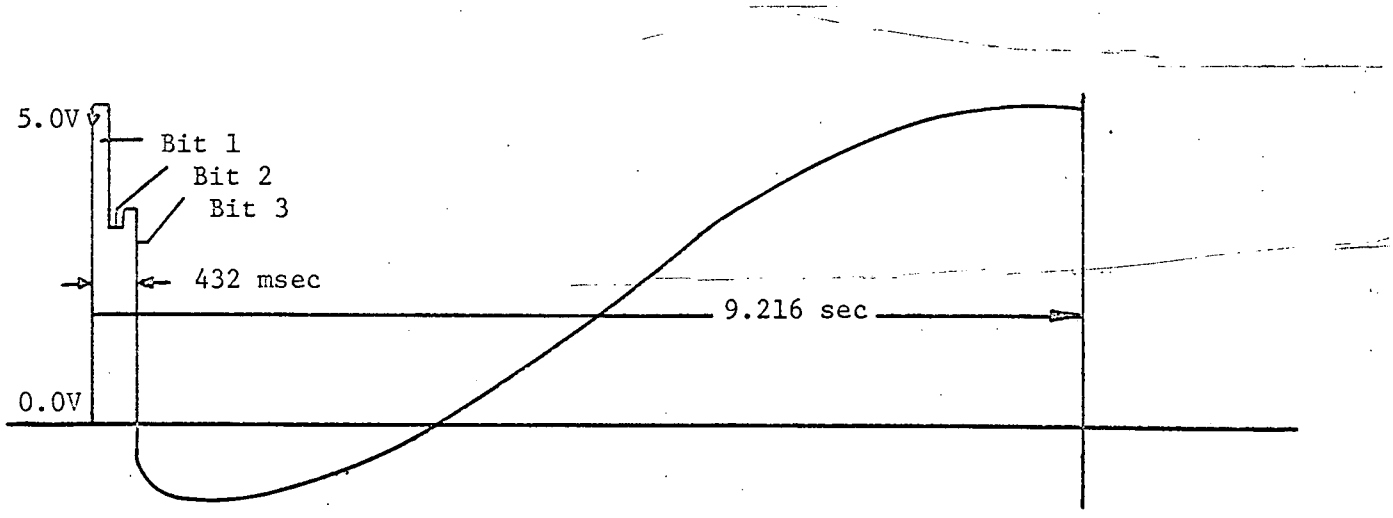

TABLE II (Concluded)

Bit 1 SYNC BIT ALWAYS 5.1 V

Bit 2 RANGE, PROBE, CALIBRATE BIT

VOLTAGE					
0.500	PANGE	4	PROBE	2	MEASURE
0.750	"	3	"	2	"
1.000	"	2	"	2	"
1.250	"	1	"	2	"
1.500	"	4	"	1	"
1.750	"	3	"	1	"
2.000	"	2	"	1	"
2.250	"	1	"	1	"
2.500	"	4	"	2	CALIBRATE
2.750	"	3	"	2	"
3.000	"	2	"	2	"
3.250	"	1	"	2	"
3.500	"	4	"	1	COMMON MODE CK
3.750	"	3	"	1	"
4.000	"	2	"	1	"
4.250	"	1	"	1	"

Bit 3 SWEEP VOLTAGE START BIT

FLIGHT UNIT:

SWEEP VOLTAGE START = 2.174 (Bit 3) - 3.620

TABLE III

SYSTEMS I AND II COMMAND STATUS INDICATIONS

SUBCOMMUTATOR OUTPUT LEVELS

VOLTAGE		FUNCTION		CMD STATUS
0.500	SYSTEM I	RESET		1 1 1
0.750	"	FAST MODE	PROBE 2 ONLY	1 1 0
1.000	"	" "	" 1 "	1 0 1
1.250	"	" "	ALTERNATE	1 0 0
1.500	"	RESET		0 1 1
1.750	"	NORMAL MODE	PROBE 2 ONLY	0 1 0
2.000	"	" "	" 1 "	0 0 1
2.250	"	" "	ALTERNATE	0 0 0
2.500	SYSTEM II	RESET		1 1 1
2.750	"	ΔV BIAS=10V		1 1 0
3.000	"	" " 8V		1 0 1
3.250	"	" " 6V		1 0 0
3.500	"	RESET		0 1 1
3.750	"	ΔV BIAS= 4V		0 1 0
4.000	"	" " 2V		0 0 1
4.250	"	" " 0V		0 0 0

3. DATA ANALYSIS

This section outlines the computer program which was developed and used to take the raw data from the decom and orbit tapes provided by the project and 1) reduce the ionospheric electron temperature and density as well as the spacecraft potential results from the F-02 experiment, and 2) to display these results along with other supporting information (e.g., angle of attack, latitude, longitude, etc.). Before discussing the program and the numerical techniques, it is appropriate to outline briefly those aspects of the theory of moving cylindrical Langmuir probes which were used by the data analysis programs to obtain atmospheric electron temperatures and densities.

3.1. Probe Characteristics

3.1.1. Infinite Probes

The classical theory describing the current collection (volt-ampere) characteristics for stationary probes of simple geometry is well-known (Mott-Smith and Langmuir, 1926). When an infinitely long cylindrical probe whose radius is less than the characteristic Debye length is immersed in a plasma, the current collected is

$$I = A_c N e \sqrt{\frac{kT}{2m\pi}} \exp(-V) \qquad v < v_p \tag{1}$$

$$I = \sqrt{\frac{kT}{2m\pi}}\, A_c N e \left(\frac{2}{\sqrt{\pi}} \sqrt{V} + e^{V} \operatorname{erfc}(\sqrt{V}) \right) \simeq A_c N e \sqrt{\frac{kT}{2m\pi}} \cdot \frac{2}{\sqrt{\pi}} (1+V)^{\frac{1}{2}} \qquad v > v_p \tag{2}$$

where $V = |e(v-v_p)/kT|$

I = current due to the species under consideration

e = electron charge

v = applied potential

v_p = space potential (plasma zero reference)

N = density

A_c = collector area

k = Boltzmann's constant

T = temperature.

This theory has been extended (Kanal, 1964) to moving probes in Maxwellian plasmas:

$$I = A_c N e \sqrt{\frac{kT}{2m\pi}} \exp[-(V+k^2)] \sum_0^\infty \frac{(2n+1)!}{(n!)^2 2^{2k}} (k/\sqrt{V})^n I_n(2k\sqrt{V}) \qquad v < v_p \qquad (3)$$

where $k = \lambda \sin\theta$

$\lambda = u/\sqrt{2kT/m}$

u = spacecraft velocity

θ = angle of attack

I_n = modified Bessel function of first kind

$$I = A_c N e \sqrt{\frac{kT}{2m\pi}} \frac{2}{\sqrt{\pi}} e^{V-k^2} \sum_0^\infty \frac{(k/\sqrt{V})^n}{n!} \Gamma(n + 3/2, V) J_n(2k\sqrt{V}) \qquad v > v_p \qquad (4)$$

where J_n is the n^{th} Bessel function and $\Gamma(n + 3/2, V)$ is the incomplete gamma function.

The OGO spacecraft orbital velocity (approximately 8 km/sec) and a mean thermal speed for electrons of approximately 300 km/sec result in a speed ratio of about 0.025. For these values of λ Equations 3 and 4 differ from Equations 1 and 2 by negligibly small amounts (0.1%). Thus the probes may be considered stationary with respect to electrons.

However, the heavier ions are moving considerably more slowly such that the speed ratio is about 4, so that the random motions of these particles are less important than the drift component. Indeed, if one ignores the thermal motion, assuming a cold ion model (the limiting model as $\lambda \to \infty$), the following equation describes the collected current ($v > v_p$)

$$I = A_c' N e \sqrt{\frac{kT}{2m\pi}} \sqrt{1 + \frac{e(v-v_p)}{U}} \tag{5}$$

where A_c' = cross-sectional area of the probe

$U = \frac{1}{2}mu^2$.

When Equation 5 is compared to Equation 4 ($\lambda = 4$), once again, the differences are negligibly small (<0.1%), so that the thermal motions of the ions may be ignored.

Thus, a complete model describing current collected by a long thin probe moving through a plasma from both ions and electrons is as follows:

$$I = A_c N e \sqrt{\frac{kT_e}{2m_e\pi}} \exp\left(\frac{e(v-v_p)}{kT}\right) - \sqrt{\frac{kT_i}{2m_i\pi}} A_c' N e \sqrt{1 + \frac{e(v_p-v)}{U}} \qquad v < v_p;\ \lambda \geq 4 \tag{6a}$$

$$I = A_c N e \left(\sqrt{\frac{kT_e}{2m_e\pi}} \exp\left(\frac{e(v-v_p)}{kT}\right) - \sqrt{\frac{kT_i}{2m_i\pi}} \frac{2}{\sqrt{\pi}} \left(1 + \frac{e(v_p-v)}{kT}\right)^{\frac{1}{2}}\right) \qquad v < v_p;\ \lambda = 0 \tag{6b}$$

$$I = A_c N e \sqrt{\frac{kT_e}{2m\pi}} \frac{2}{\sqrt{\pi}} \sqrt{1 + \frac{e(v-v_p)}{kT}} + \text{ion} \qquad v > v_p \tag{7}$$

where the ion component when $v > v_p$ is ignored, because the $v = v_p$ ion current is a factor of 50 smaller than the electron component and is decreasing as v increases.

3.1.2. Finite Probes

3.1.2.1. Retarding Region

The F-02 experiment had two probes mounted on the orbital plane experiment package so that one probe was always at 90° to the velocity vector and one at 0° to the velocity vector. The probe mounted at 90° to the velocity vector was found to conform well to the above-outlined theory when $v < v_p$. However, because of a well-known end effect, the

ion current collected by the other probe, aligned with the velocity vector, did not behave at all in accordance with Equation 4. The essence of the explanation for this phenomenon concerns the influence of the spherical sheath surrounding the tip of the finite (~9 in.) probe, through which an ion must pass before being collected.

Although this end effect has been treated in the literature and is understood qualitatively, there is no useful quantitative description of this component of the collected current which can be utilized in a data reduction scheme. Therefore, the procedure used for F-02 data from this probe was to assume a linear model which adequately describes the current:

$$I = a_1 + a_2 v + A_c N e \sqrt{\frac{kT_e}{2m_e \pi}} \exp\left(+\frac{e(v-v_p)}{kT}\right) \qquad (8)$$

Examples of the use of this model and model 6a are presented in Figure 3.

3.1.2.2. Accelerating Region

In the accelerating region for electrons ($v > v_p$, so that electrons are attracted to the probe), neither the 0° probe or the 90° probe conformed to the theory. The proposed explanation for this effect once again concerns the "finiteness" of the probe.

Unpublished work by M. Kanal has suggested that a semi-infinite cylindrical probe, i.e., a probe with one and only one end, would be described by

$$I = A_c N e \sqrt{\frac{kT}{2m\pi}} \left[\left(\sqrt{\frac{V}{\pi}} + \frac{e^V \operatorname{erfc}(\sqrt{V})}{2}\right) + \frac{1+V}{2}\right] \qquad (9)$$

The first term in Equation 9 is one-half the current which would be collected by an infinite cylinder; the second term is one-half the current which would be collected by a sphere of equivalent surface area. Figure 4 presents the theoretical normalized currents from a sphere, an infinite cylinder, Equation 9, and the result of a "best fit" power law model $(1 + V)^{\alpha}$, where $\alpha = 0.85$. It is clear that the semi-infinite cylinder model describes a probe characteristic considerably better than

the model for an infinite cylinder.

The results of computer calculations of accelerated current collected by a finite cylinder due to streams of monoenergetic charged particles indicated that, when the potential distribution about the probe was described by a simple power law, the current collected was "reasonably linear" except near space potential. Inasmuch as a Maxwellian distribution may be viewed as a superposition of a number of monoenergetic beams, it is not unreasonable to assume that the current collected due to Maxwellian particles passing through the spherical sheath about the tip of the probe might also be reasonably linear. Because of this, and for lack of a better alternative, the following model, with modified linear term, was used in the accelerating region for the finite probes aboard OGO-VI.

$$I = A_c Ne \sqrt{\frac{kT}{2m\pi}} \left[\left(\sqrt{\frac{V}{\pi}} + \frac{e^V \operatorname{erfc}(\sqrt{V})}{2} \right) + \frac{1+pV}{2} \right] \qquad (10)$$

An example of the correspondence between the data and this model is shown in Figure 5. Although the derivation of this model is empirical and somewhat arbitrary, it is far superior to the infinite cylinder, at least for the F-02 experiment.

3.2. General Program Flow

Figure 6 is a block diagram describing the program flow. The F-02 data reduction program consists of a main routine (MR) and several subroutines, MR has two major functions: 1) it acts as an interface between the person requesting data reduction and the machine, and 2) it directs the program flow to the currect subroutines, MR first checks to see of the requested outputs are consistent with each other. If not, it makes an appropriate change to whatever data is to be output. The routine then loads the subroutines needed to perform the requested data reduction. All output tapes are then put in their appropriate starting positions, and the data request to be reduced is read from cards.

MR is now ready to begin its second function. Subroutine LABEL is called to read the decom tape label of the file to be processed. The label is decoded and printed and all subroutine setup entries are called. If part of a file is to be reduced, rather than the whole file, its limits are read and the tape is moved to the starting time. Subroutine SWEEP is called to gather the next voltage sweep and resulting data curve, and the analog bits are decoded. Subroutine CALBRT is called to determine if the curve is part of a calibration sequence. If so, new calibration constants are computed and EXPPRT is called to print the ones that changed. If the curve is not a calibration curve, subroutine CONVRT is called to convert the input data to volts and amperes utilizing the standard relationship $Y = mx + b$, and this subroutine in turn calls the data reduction subroutine BILL which reduces the raw probe data to temperature. When subroutine BILL returns to CONVRT, CONVRT prints the reduced data along with selected orbital parameters (Figure 7).

When all of these subroutines return to MR the subroutine INPRT is called to print any experiment parameters which changed for this particular curve, and also to print appropriate comment about its disposition (Figure 8). At this point the program returns to get the next data sweep and this continues until the requested stop time is passed or an end-of-file condition on the input tape is detected, error conditions notwithstanding. At this point the program will reduce another file on the current tape, or on another tape, or stop, depending on the availability of another data request and its contents.

In addition to the tasks of producing numbers, the data analysis subroutines also provide for the optional display of data curves and resulting fits in four different forms. The experimenter has his choice of viewing his data and results as

1) a listing of all the raw data and computed results for each curve,
2) a printer plot of the raw data and the "residuals" from a fit,
3) a Calcomp plot of the raw data and the residuals,
4) a storage tube CRT display which can be filmed,
5) any combination of the above.

PROBE 1
RANGE 1
SYSTEM 2
VERSION 3

DAY 140
GMT 0:47:34.2
LOCAL 21:49
ORBIT 5043

ANGLE 1.7
VELOCITY 7.16
ALTITUDE 1044.1
GM LAT -19.4
LONGITUDE -45.0
SZA 149.3

TEMP 1530.
DENSITY 4.90E+03
FLT V 2.69
SPC V 3.29
QUAL 4.0
ITERS 5
PARAMS 2.56E-02
2.07E+00
2.66E-02
-1.82E+00

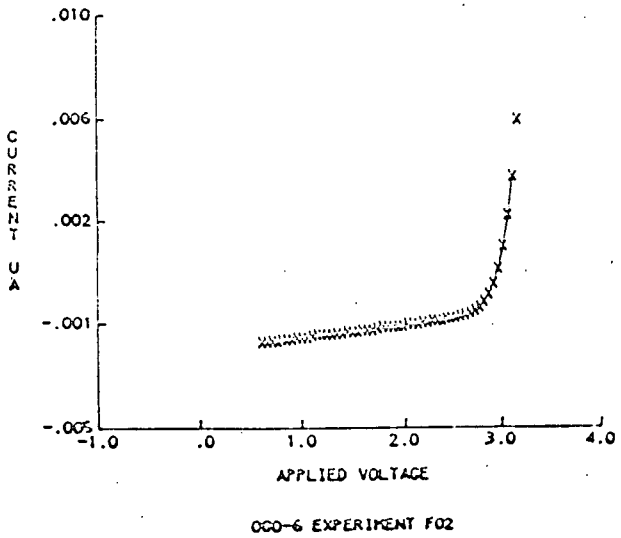

OGO-6 EXPERIMENT F02

PROBE 2
RANGE 1
SYSTEM 2
VERSION 3

DAY 140
GMT 0:48: 8.7
LOCAL 21:52
ORBIT 5043

ANGLE 1.2
VELOCITY 7.16
ALTITUDE 1045.7
GM LAT -17.5
LONGITUDE -44.6
SZA 149.9

TEMP 1820.
DENSITY .00E+00
FLT V 3.26
SPC V
QUAL 10.0
ITERS 3
PARAMS 2.51E-04
1.26E-03
1.11E-01
6.35E+00

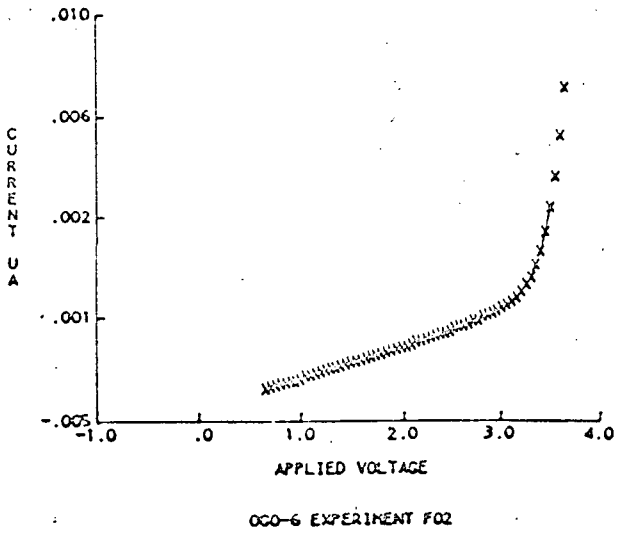

OGO-6 EXPERIMENT F02

Figure 3. Graphical program output, exhibiting retarding region data and model equations, for both probes.

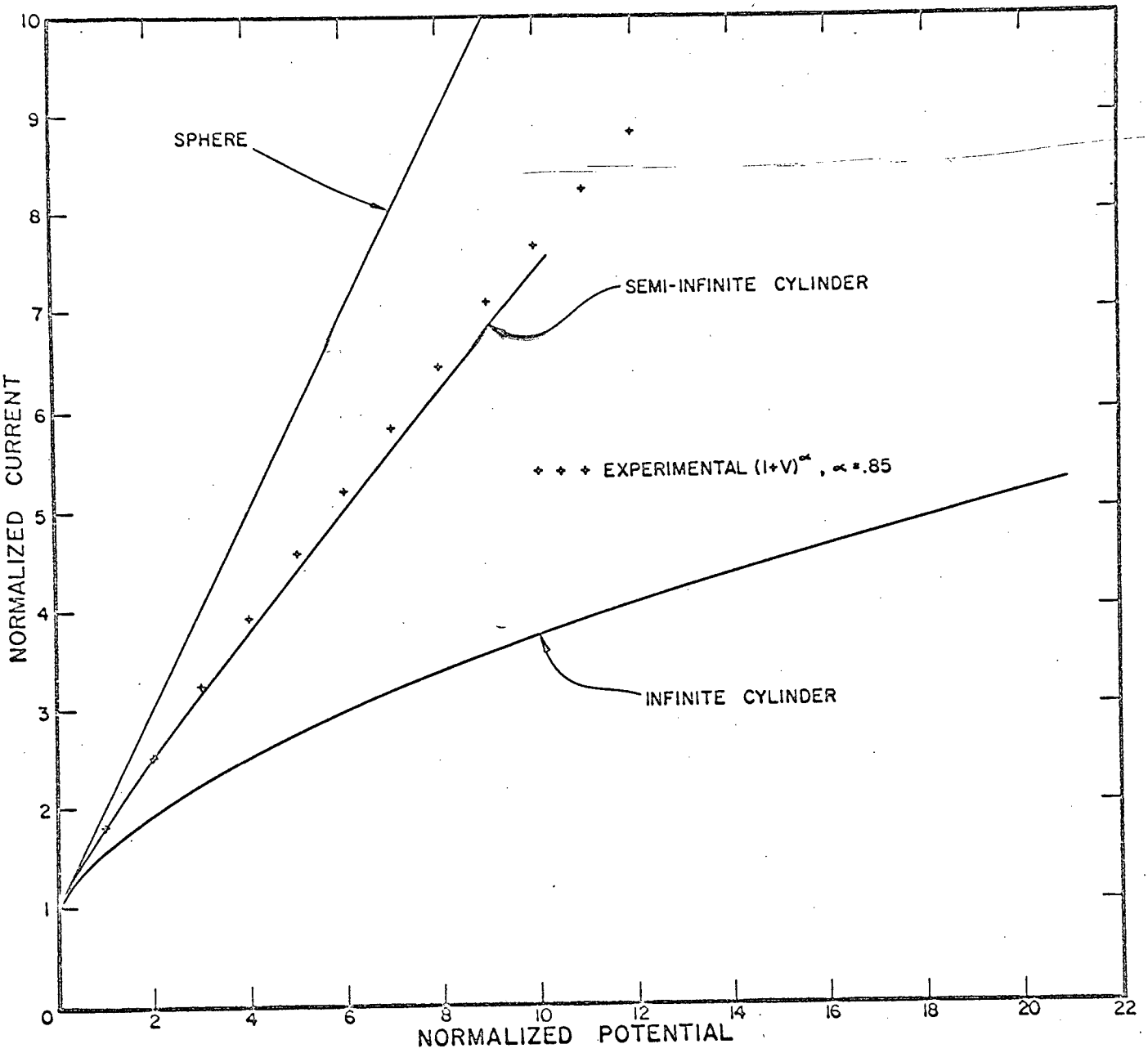

Figure 4. Theoretical normalized currents vs. normalized potential for a sphere, an infinite cylinder, Equation 9, and power law model $(1 + V)^{\alpha}$, $\alpha = 0.85$.

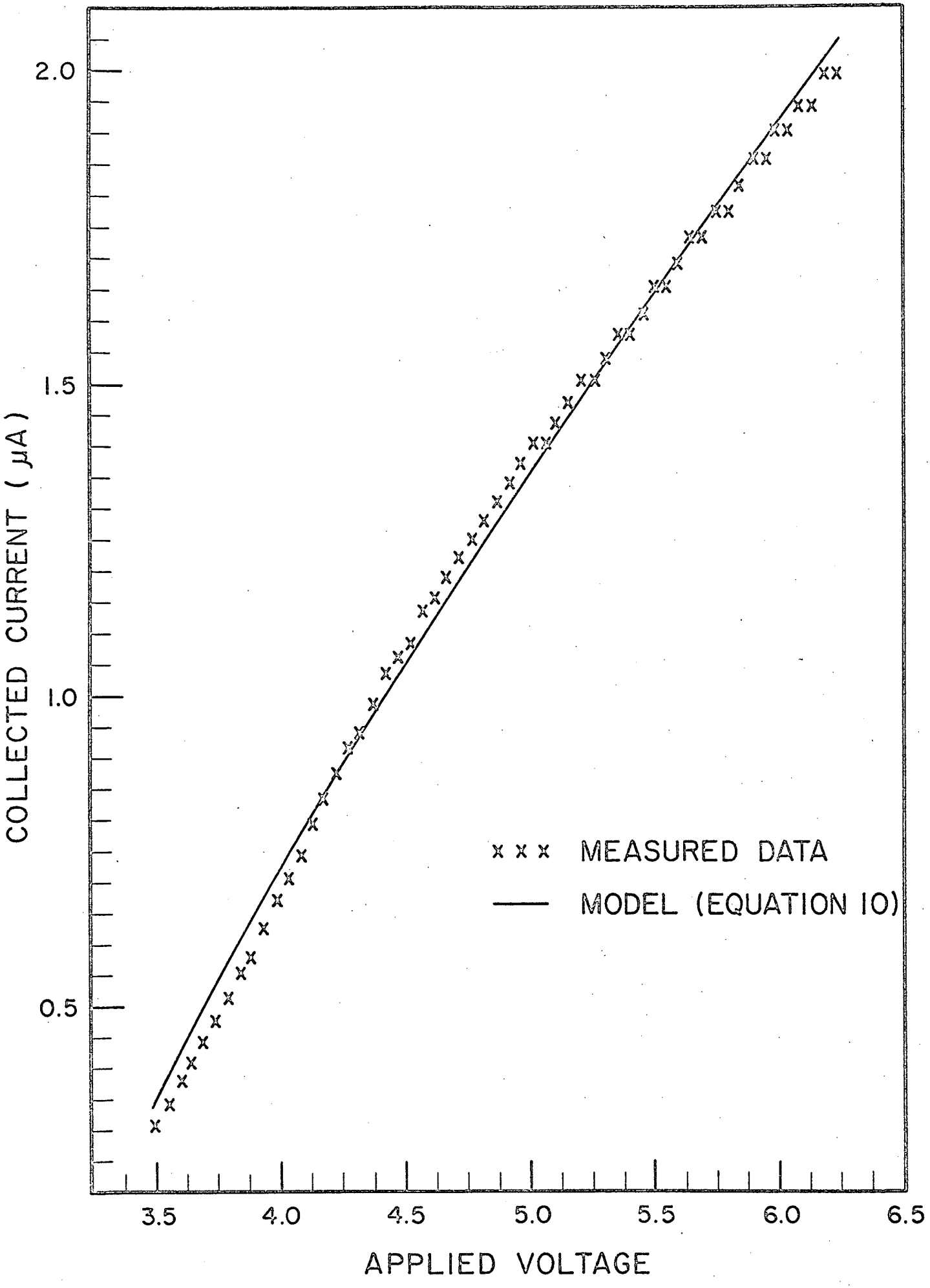

Figure 5. Comparison of Equation 10 with data.

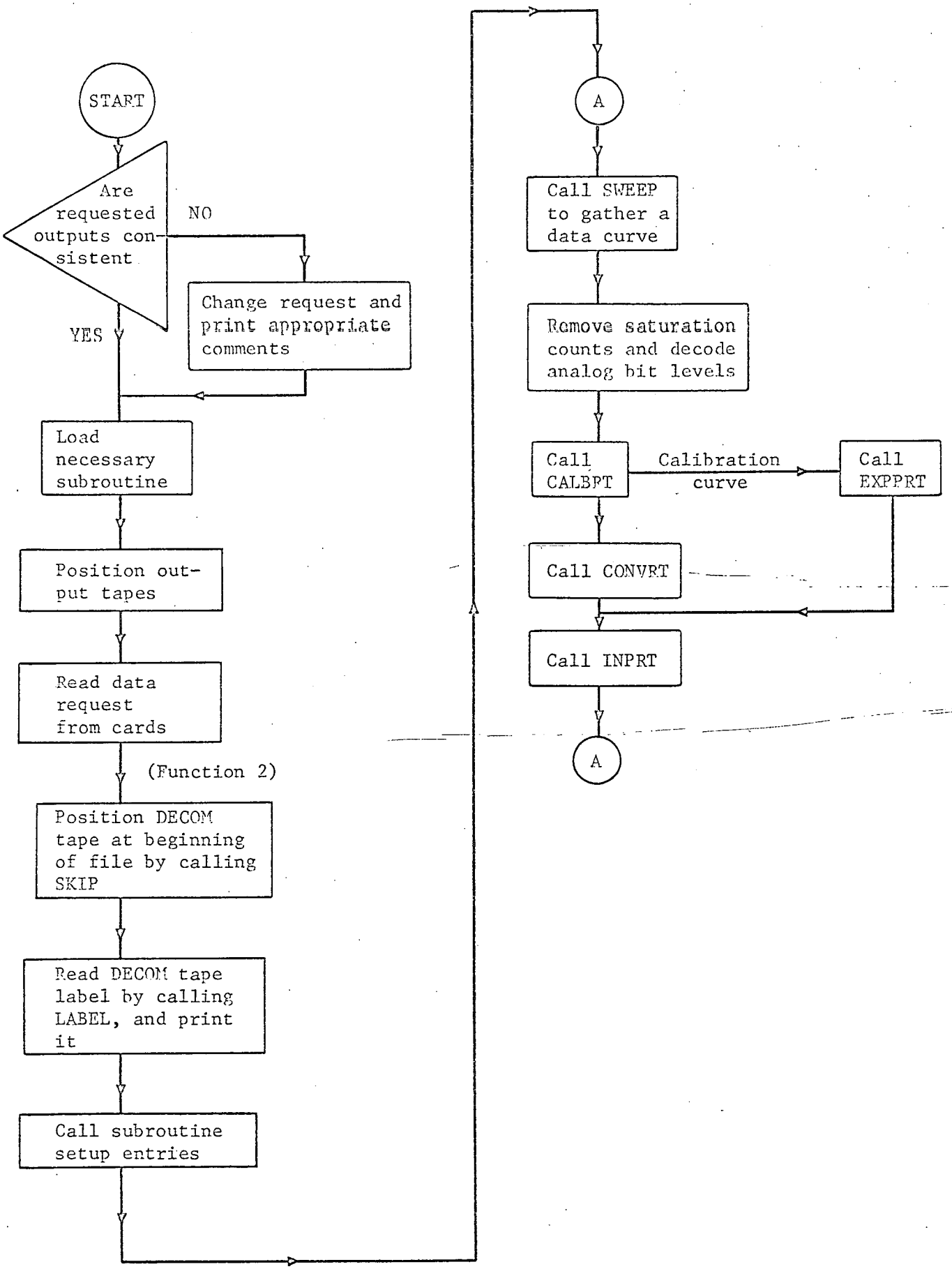

Figure 6. General program flow.

DECOM TAPE 1101 FILE 8 ORBIT 169 DAY 160 SYSTEM 2 VERSION OCB5

HR:MN:SS.SSS	P	R	LHR:LMN	TEMP	DENSITY	FLT. POT	SP. POT	QUAL	ALTITUDE	MAG LAT	GEO LAT	GEO LONG	SZA	DIPL
7: 5: 3.71	2	2	17:15	2954.7		2.51		45.98	832.33	7.46	15.05	159.90	80.53	8.04
7: 5:22.14	2	4	17:44		7.455E 04	2.69	3.66	0.40	825.92	8.53	16.13	159.99	80.28	9.07
7: 5:40.57	1	2	17:44	3233.7	1.060E 05	2.45	3.69	280.66	819.52	9.61	17.21	160.08	80.03	10.14
7: 6:17.44	2	2	17:44	3114.6		2.43		37.97	806.65	11.78	19.37	160.26	79.54	12.29
7: 6:35.87	2	4	17:46		7.349E 04	2.60	3.63	0.48	800.19	12.86	20.46	160.36	79.30	13.35
7: 6:54.30	1	2	17:46	3721.7	1.163E 05	2.61	3.77	28.67	793.72	13.94	21.54	160.45	79.06	14.40
7: 7:31.17	2	2	17:48	3269.5		2.35		29.55	780.71	16.12	23.72	160.66	78.60	16.55
7: 7:49.60	2	4	17:48		7.961E 04	2.60	3.65	0.57	774.20	17.21	24.81	160.76	78.38	17.67
7: 9:21.76	1	2	17:48	4095.8	1.412E 05	2.45	3.76	64.01	741.57	22.70	30.28	161.36	77.31	22.99
7: 9:30.97	1	3	17:53	3933.9	1.356E 05	2.47	3.71	109.56	738.31	23.25	30.83	161.42	77.21	23.52
7: 9:58.62	2	2	17:53	3536.0		2.11		34.83	728.52	24.91	32.48	161.62	76.90	25.28
7:10:17.05	2	4	17:55		8.390E 04	2.32	3.53	0.55	722.02	26.02	33.59	161.77	76.71	26.24
7:10:35.48	1	2	17:55	3466.7	1.260E 05	2.49	3.55	89.83	715.52	27.13	34.69	161.92	76.53	27.30
7:10:44.70	1	3	17:55	3839.8	1.339E 05	2.45	3.65	100.66	712.27	27.68	35.25	162.00	76.43	27.87
7:11:12.35	2	2	17:55	3533.3		2.15		33.73	702.55	29.35	36.91	162.24	76.16	29.53
7:11:21.57	2	3	17:58	3472.8		2.27		107.78	699.32	29.91	37.46	162.33	76.08	30.02
7:11:30.78	2	4	17:58		9.066E 04	2.32	3.53	0.60	696.10	30.47	38.01	162.41	75.99	30.55
7:11:49.21	1	2	17:58	3913.5	1.434E 05	2.35	3.59	62.93	689.64	31.58	39.12	162.59	75.82	31.73
7:11:58.43	1	3	17:58	4016.2	1.435E 05	2.40	3.65	136.37	686.42	32.14	39.68	162.67	75.73	32.39
7:12:26.08	2	2	18: 2	3599.9		2.11		26.97	676.84	33.82	41.35	162.98	75.50	33.86
7:12:35.29	2	3	18: 2	3362.5		2.25		101.31	673.65	34.38	41.91	163.08	75.42	34.42
7:12:44.51	2	4	18: 2		9.827E 04	2.27	3.49	0.55	670.46	34.95	42.46	163.18	75.34	35.03
7:13:12.16	1	3	18: 2	4029.8	1.711E 05	2.32	3.59	81.94	660.95	36.63	44.14	163.51	75.12	36.75
7:13:39.80	2	2	18: 5	3613.6		2.04		34.00	651.52	38.33	45.81	163.87	74.92	38.39
7:13:49.02	2	3	18: 5	3566.2		2.18		94.75	648.38	38.89	46.37	163.99	74.85	39.05
7:13:58.24	2	4	18: 5		1.044E 05	2.23	3.45	0.51	645.23	39.45	46.93	164.11	74.78	39.77
7:14:16.67	1	2	18: 5	3906.9	1.620E 05	2.22	3.45	21.87	639.05	40.59	48.05	164.40	74.66	40.73
7:14:25.89	1	3	18: 9	3991.9	1.683E 05	2.23	3.49	101.50	635.97	41.15	48.61	164.54	74.61	41.26
7:14:53.54	2	2	18: 9	3563.2		1.96		49.75	626.71	42.86	50.29	164.98	74.43	43.22
7:15: 2.75	2	3	18: 9	3450.7		2.08		104.57	623.65	43.42	50.85	165.13	74.38	43.90
7:15:11.96	2	4	18:14		1.005E 05	2.18	3.32	0.61	620.63	43.99	51.41	165.31	74.33	44.34
7:15:30.40	1	2	18:14	3892.9	1.866E 05	2.12	3.36	30.65	614.60	45.13	52.53	165.66	74.23	45.41
7:15:39.61	1	3	18:14	3888.4	1.926E 05	2.13	3.37	86.00	611.58	45.70	53.09	165.84	74.18	46.06
7:16: 7.26	2	2	18:14	3565.3		1.85		62.96	602.60	47.42	54.77	166.40	74.04	48.10
7:16:16.48	2	3	18:20	3626.4		1.98		86.64	599.66	47.99	55.33	166.62	74.01	48.56
7:16:53.34	1	3	18:20	3758.1	2.293E 05	2.00	3.19	76.91	587.92	50.28	57.57	167.50	73.85	51.27
7:17:30.21	2	3	18:27	3342.0		1.87		56.94	576.47	52.59	59.81	168.58	73.74	53.54
7:19:20.80	1	3	18:27	3641.0	3.374E 05	1.82	2.97	89.03	543.49	59.53	66.47	173.01	73.54	61.53
7:19:57.66	2	3	18:45	3293.6		1.61		107.77	532.98	61.86	68.66	175.00	73.52	64.91
7:20:34.53	1	3	18:59	3965.1	1.793E 05	1.78	2.99	177.00	522.92	64.19	70.81	177.76	73.55	66.84
7:21: 2.18	2	2	18:59	3532.4		1.55		107.98	515.43	65.95	72.41	166.99	73.58	69.83
7:21:11.39	2	3	19:19	3140.6		1.78		118.74	513.06	66.53	72.92	112.75	73.60	69.94
7:22:25.12	2	3	19:19	3301.7		1.71		107.26	494.48	71.24	76.88	-168.96	73.78	74.63
7:23: 1.98	1	3	19:47	3750.4	2.264E 05	1.81	2.95	86.86	485.60	73.59	78.71	-162.13	73.91	78.79
7:23:38.85	2	3	20:31	3093.1		1.69		69.01	477.30	75.96	80.15	-151.42	74.09	79.30
7:24:52.57	2	3	21:42	3181.4		1.65		87.17	461.64	80.71	81.90	-122.97	74.50	83.51
7:26: 6.30	2	3	23:35	3160.9		1.64		80.59	447.71	85.47	81.06	-91.31	75.03	84.45
7:27:20.03	2	3	1:12	3197.5		1.60		72.70	435.66	88.33	78.09	-70.30	75.68	80.21
7:29:10.62	1	3	2:29	3794.0	3.355E 05	1.70	2.89	82.17	421.00	82.52	72.10	-54.11	76.84	75.19
7:29:47.48	2	3	3:48	3154.3		1.59		85.19	417.14	80.11	69.90	-51.08	77.28	73.06
7:30:24.35	1	3	3:48	3870.0	2.521E 05	1.69	2.93	93.59	413.83	77.69	67.65	-48.65	77.74	70.64
7:31: 1.21	2	3	4: 9	3376.7		1.66		254.63	410.84	75.28	65.37	-46.54	78.22	69.55
7:31:38.08	1	3	4:24	3927.1	1.722E 05	1.71	2.94	160.80	408.69	72.86	63.05	-44.98	78.72	66.53
7:32: 5.73	2	2	4:24	3634.5		1.53		150.86	407.21	71.04	61.31	-43.87	79.11	65.44
7:32:14.94	2	3	4:35	3680.3		1.64		155.07	406.90	70.43	60.72	-43.57	79.25	64.52

Figure 7. Sample of reduced data output.

S/C PARAMETERS

TAPE 1101 FILE 8 BIT RATE 8 ORBIT 169 DAY 168 SYSTEM 2 COMMAND STATUS 2 EQUIPMENT GROUP 2

HH:MM:SS.SSS	S/C CLOCK	RNG	PRB	MODE	N	F1	F3	ANGLE	SAI	ACC	GJS	NO	SP	COMMENT
7:38: 5.148	30283139	1	2	CAL	98	0	3	16.98	90.25	30.86	0	0	0	CALBRT-SYSTEM 2:GAIN
7:38:14.367	30283147	2	2		122									CALBRT-SYSTEM 2:GAIN
7:38:23.582	30283155	3	2											CALBRT-DELTA V
7:38:32.797	30283163	4	2											CALBRT-SYSTEM 2:GAIN
7:38:42.016	30283171	1	1	MEAS	98									NOT ENOUGH DATA POINTS
7:38:51.230	30283179	2	1		122									NOT ENOUGH DATA POINTS
7:39: 0.445	30283187	3	1					1.57						ITERATION DID NOT CONVERGE
7:39: 9.660	30283195	4	1					2.09						NOT ENOUGH DEFLECTION
7:39:18.879	30283203	1	2					16.98						NOT ENOUGH DATA POINTS
7:39:28.094	30283211	2	2		104									NOT ENOUGH DATA POINTS
7:39:37.309	30283211	2	2											CURVE MISSED:BIT1 IS MISSING
7:39:46.527	30283227	4	2		121			2.27						NOT ENOUGH DEFLECTION
7:39:55.742	30283235	1	1		122			16.98		30.72				NOT ENOUGH DATA POINTS
7:40: 4.957	30283243	2	1		102									NOT ENOUGH DATA POINTS
7:40:14.176	30283243	2	1											CURVE MISSED:BIT1 IS MISSING
7:40:23.391	30283259	4	1		121			2.43		30.86		32		NOT ENOUGH DEFLECTION
7:40:32.605	30283267	1	2		122			16.98						NOT ENOUGH DATA POINTS
7:40:41.820	30283275	2	2		98									NOT ENOUGH DATA POINTS
7:40:51.039	30283283	3	2		122			2.00						TEMPERATURE CURVE
7:41: 0.254	30283291	4	2					1.46				0		NOT ENOUGH DEFLECTION
7:41: 9.469	30283299	1	1					16.98						NOT ENOUGH DATA POINTS
7:41:18.687	30283307	2	1											NOT ENOUGH DATA POINTS
7:41:27.902	30283315	3	1		114			2.45						ITERATION DID NOT CONVERGE
7:41:37.117	30283315	3	1											CURVE MISSED:BIT1 IS MISSING
7:41:46.336	30283315	3	1											CURVE MISSED:BIT1 IS MISSING
7:41:55.551	30283339	2	2		97			16.55						NOT ENOUGH DATA POINTS
7:42: 4.766	30283347	3	2		122			1.76						TEMPERATURE CURVE
7:42:13.980	30283355	4	2					2.18						DENSITY CURVE
7:42:23.199	30283363	1	1					16.98						NOT ENOUGH DATA POINTS
7:42:32.414	30283371	2	1					2.43						TEMPERATURE & DENSITY CURVE
7:42:41.629	30283379	3	1					2.31						ITERATION DID NOT CONVERGE
7:42:50.848	30283387	4	1					2.02						NOT ENOUGH DEFLECTION
7:43: 0.063	30283395	1	2					16.98						NOT ENOUGH DATA POINTS
7:43: 9.277	30283403	2	2					1.99						TEMPERATURE CURVE
7:43:18.492	30283411	3	2					2.26						TEMPERATURE CURVE
7:43:27.711	30283419	4	2					2.37						DENSITY CURVE
7:43:36.926	30283427	4	2		98									CURVE LESS THAN 2 COUNTS
7:43:46.141	30283435	2	1		122			2.14						TEMPERATURE & DENSITY CURVE
7:43:55.359	30283443	3	1					1.76		30.72				ITERATION DID NOT CONVERGE
7:44: 4.574	30283451	4	1					1.75						NOT ENOUGH DEFLECTION
7:44:13.789	30283459	1	2					16.98		30.86				NOT ENOUGH DATA POINTS
7:44:23.008	30283467	2	2					2.32						TEMPERATURE CURVE
7:44:32.223	30283475	3	2					2.35						NOT ENOUGH DEFLECTION
7:44:41.438	30283483	4	2					2.25						DENSITY CURVE
7:44:50.652	30283491	1	1					16.98						NOT ENOUGH DATA POINTS
7:44:59.871	30283499	2	1		98									NOT ENOUGH DATA POINTS
7:45: 9.086	30283507	3	1		122			2.16						NOT ENOUGH DEFLECTION
7:45:18.301	30283515	4	1					2.56						NOT ENOUGH DEFLECTION
7:45:27.520	30283523	1	2					17.84						NOT ENOUGH DATA POINTS
7:45:36.734	30283531	2	2					2.85						ITERATION DID NOT CONVERGE
7:45:45.949	30283539	3	2		98			2.78						NOT ENOUGH DEFLECTION
7:45:55.168	30283547	4	2		118			2.57						DENSITY CURVE
7:46: 4.383	30283547	4	2											CURVE MISSED:BIT1 IS MISSING
7:46:13.598	30283563	2	1		121			3.12						TEMPERATURE & DENSITY CURVE

Figure 8. Spacecraft parameters.

3.3. Data Fitting Technique

Once raw data has been gathered from decom tapes and converted to voltages and current, subroutines BILL and either TMPRTR, TMPBI, or DENSTY are called to obtain values for the atmospheric parameters, density, temperature, and space potential. The technique applied can be called "Least Squares Fitting," "Maximum Likelihood Estimation," or "Nonlinear Regression." In any case the data collected during a voltage sweep are viewed as a random sample from a probability density whose mean is a function of applied voltage which we refer to as a "model". Thus:

$$Y_i \sim N(f(\hat{a},v_i),\sigma^2)$$

or

$$Y_i = f(\hat{a},v_i) + \varepsilon_i \qquad \varepsilon_i \sim N(0,\sigma^2)$$

where Y_i is a random variable representing current collected at voltage v_i

v_i is the voltage applied to the probe

ε_i is a random variable representing the "error" or noise associated with the observation of current Y_i

σ^2 is the variance of the noise distribution

$\sim N(u,\sigma^2)$ means normally distributed with mean u and variance σ^2

$\hat{a}$ is a vector of parameters to the model

$f(\hat{a},v_i)$ is the modeling function, or a form which the data would follow as a function of voltage in the absence of noise, according to the best available theory (Equations 6a, 8, and 10).

Estimates of the parameters to the model are computed by assuming that the proper values are those which would make the observed "random sample" the most likely one. In the event that the "errors" are normally distributed this condition is equivalent to a least squared error criterion, which is useful even when errors are not normally distributed. Thus statistics for the atmospheric parameters are calculated by finding the vector $\hat{a}$ such that

$$\phi = \sum_{i=1}^{n} (Y_i - f(\hat{a}, v_i))^2 = \min$$

or

$$\frac{\partial \phi}{\partial a_j} = -2 \sum_{i=1}^{n} (Y_i - f(\hat{a}, v_i)) \frac{\partial f(\hat{a}, v_i)}{\partial a_j} = 0 \qquad j = 1, \cdots, m$$

where m is the number of unknown parameters to the model and n is the number of observations of current and voltage in the random sample.

Because of the nature of the models for current collected by the F-02 probe, the above system of equations is intrinsically nonlinear. Hence an iterative numerical technique must be used. The one chosen here is a modified Newton's method for systems of nonlinear equations which is implemented by subroutine STNLSE. It is equivalent to the "Linearization" of the nonlinear model on an iterative basis. Although more specialized techniques have been applied to probe data (Theis, 1968), this approach is used because it is more general (three different models are used), it converges slightly faster, is easily modified, and does not entail a significant amount of extra computation.

In order to prevent an inadequate model in the accelerating region from biasing the results obtained from a good model in the retarding region, the two regions were reduced separately. The algorithm used to locate these two regions takes advantage of the fact that the difference between space potential (v_p) and the floating potential (or zero current potential, which is the most salient feature of a data curve) when expressed in units of normalized potential (i.e., multiplied by e/kT_e) is theoretically a weak function of temperature with a value of approximately 2. Thus the floating potential is determined and the voltage equivalent of 1.2 units of normalized potential at a temperature which is an average of the three previous temperatures is added. Then all data from the beginning of the voltage sweep to this voltage are considered to be the retarding region:

$$\{(Y_i, v_i) | v_s \leq v_i \leq v_{fl} + 1.2\ kT/e\} = \text{retarding region}$$

where I = instantaneous current at voltage v_i

v_s = first voltage in sweep

v_i = instantaneous voltage at index i

v_{fl} = voltage such that $Y(v_{fl}) = 0$

T = average of three previous temperatures

k = Boltzmann's constant

e = charge on an electron

Similarly, the accelerated region is defined as:

$$\{(Y_i, v_i) \mid v_{fl} + \frac{3.2kT}{e} < v_i < v_e \} = \text{retarding region}$$

where v_e = last voltage in sweep.

3.4. Error Estimates

Since the least squares estimates used to determine values for the atmospheric parameters in the above models are themselves random variables, they have complicated probability distributions whose variances can be estimated. These variances are quite useful as error estimates because they can be used to establish confidence intervals for temperature estimates at any desired level of risk. However, since the models are nonlinear, the level of risk can only be approximated and is accurate only to the extent that the model can be considered linear within the confidence interval. Nevertheless, approximate error estimates are almost as useful as accurate ones, and are certainly more useful than none at all. Therefore, subroutine STDERR was used on all temperature fits to calculate the variance of the model parameter from which temperature is computed. From this variance, the width of an approximate 80% confidence interval in units of degrees Kelvin was calculated. This number is returned along with computed temperatures to the main program and provides a convenient indicator of data quality.

4. RESULTS

A preliminary version of the data analysis program was operational on the Goddard Space Flight Center computer at the time of launch, and therefore some near-real-time data analysis was carried out during the first ten days of the satellite's lifetime.

The first presentation of data from the F-02 experiment was given informally at the December 1969 AGU Meeting. A special session of the 1970 National AGU Meeting held in Washington D.C. was devoted to presentations of early results from the OGO-VI satellite, and a paper on F-02 results from June 1969 was presented at that session (Samir, Nagy, and Brace, 1970). At the April 1971 National AGU Meeting another special session was organized for the presentation of OGO-VI data, this time for data related to the geomagnetic storm of November 1969. Results from the F-02 Langmuir probe experiment were presented in two of the papers (Reber, et al., 1971; Hanson, et al, 1971).

The winter predawn enhancement of the 6300 Å oxygen red line emission and the electron temperature has received a great deal of attention in the last few years. The F-02 experiment along with the F-03 ion trap experiment have provided excellent information on the electron temperature increase and on the integrated intensity of conjugate photoelectrons. These results have been presented at the April 1971 National AGU Meeting by Sanatani, et al. (1971).

The most recent theory of red arc formation is that given by Cornwall, Coroniti, and Thorne (1970), who suggest that the ring current protons generate ion cyclotron waves in the plasmapause region, and that a fraction of this wave energy is transferred to plasmaspheric electrons via Landau damping. This energy, via thermal conduction, is transported down to the ionosphere causing the red line emission. The OGO-VI satellite carried a complement of experiments capable of measuring atmospheric parameters that are relevant and necessary for a complete understanding of the processes involved in the formation of a red arc. Because of a number of factors (e.g. spacecraft potential problems, infrequent red arc occurrences, etc.), only one red arc has been studied in detail, the results of which have been presented (Nagy, et al., 1972a), and published (Nagy, et al., 1972b).

The OGO-VI experimental results were in excellent agreement with all aspects of the theory with the possible exception of the proposed wave-particle interaction mechanism.

Discrepancies between electron temperatures measured by Langmuir probes and radar backscatter techniques have been noted in recent years (e.g. Carlson and Sayers, 1970). A concentrated effort was made to study this discrepancy with the aid of the F-02 probe experiment. All the available comparison points between electron temperatures measured by the F-02 probe and the various backscatter stations, as well as the ion temperature comparisons between the F-03 ion trap and backscatter data, have been collected, The results of these comparisons have been presented (Nagy, et al., 1971), and published (McClure, et al., 1972). The average discrepancy between the probe and radar-deduced electron temperatures was found to be about 12%, or less than most of the previous comparisons. There were insufficient statistics available to subdivide the data according to important theoretical parameters (e.g. probe diameter—Debye length ratio, temperature, etc.) and therefore no clear conclusions regarding the reason for the discrepancy were possible.

Electron and ion temperature results from the F-02 and F-03 experiments, respectively, have shown very significant temperature minima in the nighttime equatorial region at altitudes above about 500 km. A great deal of effort was made to ascertain that these unexpected temperature minima were real and not a result of instrumental effects. When the integrity of the data was established it became clear that these low electron and ion temperatures are indications of the hitherto unexpected importance of adiabatic cooling of the plasma in the equatorial region. The results of these observations and the related theory are in the process of being published (Hanson, Nagy, and Moffett, 1972), and further work on this subject is in progress. Simultaneous electron and ion temperature observations by F-02 and F-03 have indicated also that ion temperatures may exceed electron temperatures at night (Hanson, Nagy, and Moffett, 1972), due to the higher electron thermal conductivity as pointed out earlier by Nagy, Bauer, and Fontheim (1968).

5. FUTURE ACTIVITIES

In order to "minimize cost and maximize science" the data reduction has proceeded on a very selective basis. Data from some selected orbits are being reduced at the moment to study the equatorial adiabatic cooling phenomenon further. It is also anticipated that studies of the angle of attack behavior of the probes will be carried out in the near future. The Langmuir probe experiments on the ESRO-1A satellite have indicated that the electron temperature is not isotropic in the nighttime midlatitude ionosphere at higher altitudes. An attempt will be made to see whether this phenomenon can be studied with data from the F-02 experiment.

6. REFERENCES

Brace, L. H., N. W. Spencer, and G. R. Carignan, "Ionsophere Electron Temperature Measurements and Their Implications," J. Geophys. Res., 68, 5397-5412, 1963.

Brace, L. H., G. R. Carignan, and J. A. Findlay, "Evaluation of Ionospheric Electron Temperature Measurements by Cylindrical Electrostatic Probes," Space Research XI, Academie-Verlag, Berlin, 1079-1105, 1971.

Carlson, H. C., and J. Sayers, "Concerning the Discrepancy in Electron Temperatures Deduced from Langmuir Probes and from Incoherent Scatter Radars," J. Geophys. Res., 75, 4883-4886, 1970.

Cornwall, J. M., F. V. Coroniti, and R. M. Thorne, "Turbulent Loss of Ring Current Protons," J. Geophys. Res., 75, 4699-4709, 1970.

Hanson, W. B., A. F. Nagy, and R. J. Moffett, "OGO-6 Measurements of Supercooled Plasma in the Equatorial Exosphere," to be published in J. Geophys. Res., 1972.

Hanson, W. B., A. F. Nagy, and R. E. Sweeney, "Geomagnetic Storm of 1969 November: Equatorial Phenomena," paper presented at the Spring Annual Meeting of the American Geophysical Union, Washington, D.C., April 1971.

Kanal, M., "Theory of Current Collection of Moving Cylindrical Probes," J. Appl. Phys., 35, 1697-1703, 1964.

McClure, J. P., W. B. Hanson, A. F. Nagy, R. J. Cicerone, L. H. Brace, M. Baron, P. Bauer, H. C. Carlson, J. V. Evans, G. N. Taylor, and R. F. Woodman, "Comparison of T_e and T_i from OGO-6 and from Various Incoherent Scatter Radars," to be published in J. Geophys. Res., 1972.

Mott-Smith, H. M., and I. Langmuir, "Theory of Collectors in Gaseous Discharges," Phys. Rev., 28, 727-763, 1926.

Nagy, A. F., P. Bauer, and E. G. Fontheim, "Nighttime Cooling of the Protonosphere," J. Geophys. Res., 73, 6259-6274, 1968.

Nagy, A. F., L. H. Brace, G. R. Carignan, and M. Kanal, "Direct Measurements Bearing on the Extent of Thermal Nonequilibrium in the Ionosphere," J. Geophys. Res., 68, 6401-6412, 1963.

Nagy, A. F., R. J. Cicerone, L. H. Brace, M. Baron, P. Bauer, H. C. Carlson, J. V. Evans, and R. F. Woodman, "Electron Temperaures Measured Simultaneously by OGO-VI Probes and Incoherent-Scatter Radars," paper presented at the Fall Annual Meeting of the American Geophysical Union, San Francisco, December 1971.

Nagy, A. F., W. B. Hanson, T. L. Aggson, and R. J. Hoch, "Satellite and Ground-Based Observations of a Red Arc," paper presented at the Spring Annual Meeting of the American Geophysical Union, Washington, D.C., April 1972a.

Nagy, A. F., W. B. Hanson, R. J. Hoch, and T. L. Aggson, "Satellite and Ground-Based Observations of a Red Arc," J. Geophys. Res., 77, 3613-3617, 1972b.

Reber, C. A., W. B. Hanson, A. F. Nagy, and D. R. Taeusch, "Geomagnetic Storm of 1969 November: Temperature and Composition Effects," paper presented at the Spring Annual Meeting of the American Geophysical Union, Washington, D.C., April 1971.

Samir, U., A. F. Nagy, and L. H. Brace, "Electron Temperature and Density from the OGO-VI Satellite," paper presented at the Spring Annual Meeting of the American Geophysical Union, Washington, D.C., April 1970.

Sanatani, S., W. B. Hanson, and A. F. Nagy, "Heating in the Nighttime Ionosphere by Conjugate Photoelectrons," paper presented at the Spring Annual Meeting of the American Geophysical Union, Washington, D.C., April 1971.

Spencer, N. W., L. H. Brace, G. R. Carignan, D. R. Taeusch, and H. B. Niemann, "Electron and Molecular Nitrogen Temperature and Density in the Thermosphere," J. Geophys. Res., 70, 2665-2698, 1965.

Taylor, H. A., Jr., L. H. Brace, H. C. Brinton, and C. R. Smith, "Direct Measurements of Helium and Hydrogen Ion Concentration and Total Ion Density to an Altitude of 940 Kilometers," J. Geophys. Res., 68, 5339-5347, 1963.

Theis, R. F., Computer Derivation of Geophysical Data from Satellite Electrostatic Probe Measurements, X-621-68-481, Goddard Space Flight Center, Greenbelt, Maryland, 1968.